

ADI schemes for pricing American options under the Heston model

Tinne Haentjens* and Karel J. in 't Hout*

October 31, 2018

Abstract

In this paper a simple, effective adaptation of Alternating Direction Implicit (ADI) time discretization schemes is proposed for the numerical pricing of American-style options under the Heston model via a partial differential complementarity problem. The stability and convergence of the new methods are extensively investigated in actual, challenging applications. In addition a relevant theoretical result is proved.

Key words: Alternating Direction Implicit schemes, American option pricing, Heston model, linear complementarity problem, Ikonen–Toivanen splitting.

1 Introduction

This paper is concerned with the numerical valuation of American-style options. We consider the adaptation of the well-known class of Alternating Direction Implicit (ADI) time discretization schemes. These splitting schemes have proven to be highly efficient, stable and robust in the numerical pricing of European-style options via multidimensional partial differential equations (PDEs). A study of their potential for American-style options is still in its infancy, however. In the present paper we propose and analyze an effective adaptation of ADI schemes to the pricing of this important type of options. For the underlying asset price process the popular Heston stochastic volatility model [15] is considered.

Let $u(s, v, t)$ be the fair value of a vanilla American put option under the Heston model if at t time units before the given maturity time the underlying asset price equals $s \geq 0$ and its variance equals $v \geq 0$. The Heston spatial differential operator \mathcal{A} applied to the function u is denoted by

$$\mathcal{A}u = \frac{1}{2}s^2v \frac{\partial^2 u}{\partial s^2} + \rho\sigma sv \frac{\partial^2 u}{\partial s \partial v} + \frac{1}{2}\sigma^2v \frac{\partial^2 u}{\partial v^2} + rs \frac{\partial u}{\partial s} + \kappa(\eta - v) \frac{\partial u}{\partial v} - ru \quad (s > 0, v > 0). \quad (1.1)$$

Here parameter $\kappa > 0$ is the mean-reversion rate, $\eta > 0$ is the long-term mean, $\sigma > 0$ is the volatility-of-variance, $\rho \in [-1, 1]$ is the correlation between the two underlying Brownian motions and r is the risk-neutral interest rate. We note that in the literature it is sometimes assumed that the so-called Feller condition $2\kappa\eta > \sigma^2$ is fulfilled, but in this paper we shall make no such assumption. Let $K, T > 0$ be the given strike price and maturity time of the American put option and denote the payoff function by

$$\phi(s) = \max(K - s, 0) \quad (s \geq 0). \quad (1.2)$$

It is well-known that the option value function u satisfies the following so-called *partial differential complementarity problem (PDCP)*:

$$\frac{\partial u}{\partial t} \geq \mathcal{A}u, \quad u \geq \phi, \quad (u - \phi) \left(\frac{\partial u}{\partial t} - \mathcal{A}u \right) = 0, \quad (1.3)$$

*Department of Mathematics and Computer Science, University of Antwerp, Middelheimlaan 1, B-2020 Antwerp, Belgium. Email: {tinne.haentjens,karel.inthout}@uantwerpen.be.

valid pointwise for (s, v, t) with $s > 0$, $v > 0$, $0 < t \leq T$. The Heston PDCP (1.3) is complemented with initial and boundary conditions. The initial condition is $u(s, v, 0) = \phi(s)$ (for $s \geq 0$, $v \geq 0$). Boundary conditions are given in Section 2 below.

The three conditions in (1.3) naturally induce a decomposition of the (s, v, t) -space: the continuation region is the set of all points (s, v, t) where the equality $\partial u / \partial t = \mathcal{A}u$ holds (and the option is held); the exercise region is the set of all points (s, v, t) where the equality $u = \phi$ holds (and the option is exercised). The joint boundary of these two regions is called the free boundary or exercise boundary. Both the option value function u and the free boundary are unknown in closed form. Further, even though no rigorous proof appears to be available at present, the function u is expected to suffer from a lack of smoothness on the free boundary, as in the Black–Scholes case.

The numerical solution of the Heston PDCP for American-style option prices has already been considered by various authors in the literature. We give here a brief overview of the main contributions.

Clarke & Parrott [7] apply finite difference schemes for the spatial discretization of (1.3) followed by the θ -method for the time discretization. This gives rise to a fully discrete linear complementarity problem (LCP) that needs to be solved in every time step. As it turns out, the common projected SOR method (see e.g. [33, 37]) is often too slow for the Heston LCP and in [7] the authors propose a multigrid method. It is based on the projected full approximation scheme (PFAS) by Brandt & Cryer [4].

Oosterlee [29] provides a detailed Fourier analysis of the PFAS approach for the Heston LCP and concludes, in particular, that an alternating line smoother is robust. For the time discretization the second-order backward differentiation formula (BDF2) was used in [29].

Toivanen & Oosterlee [34] present a projected algebraic multigrid method for LCPs and show that this is faster than geometric multigrid in the case of the Heston LCP.

Zvan, Forsyth & Vetzal [39] view the American option pricing problem as a nonlinear Heston PDE, where the early exercise constraint is incorporated by a penalty method. After spatial discretization, by finite element/volume schemes, and time discretization, by the θ -method, they obtain a nonlinear system of algebraic equations that is numerically solved through an approximate Newton method with a preconditioned CGSTAB iteration. The penalty method is shown to yield the Heston LCP as the penalty parameter tends to infinity.

Ikonen & Toivanen [24] propose splitting methods for the time discretization of the semidiscretized Heston PDCP. The methods under consideration can be viewed as analogues of well-known fractional step methods or locally one-dimensional (LOD) methods for systems of ordinary differential equations. In particular, the symmetric Strang-type splitting is adapted to the semidiscretized Heston PDCP. This leads to five LCPs per time step, each with a tridiagonal matrix. These simple LCPs are then exactly solved by the efficient Brennan–Schwartz algorithm, introduced in [5] for pricing American options under the (one-dimensional) Black–Scholes model. We remark that, since the methods in [24] are based on LOD methods, special attention must be given to the treatment of the PDCP boundary conditions, otherwise order reduction might occur. Further, the Brennan–Schwartz algorithm is only applicable under restrictive assumptions on the spatial discretization as well as (the shape of) the free boundary for the option price.

Somewhat related to [24], Villeneuve & Zhanette [36] previously formulated two adaptations of the original Peaceman–Rachford ADI scheme [30] to the semidiscretized PDCP from the pricing of American options on two assets under the Black–Scholes model. These authors first perform a coordinate transformation, so as to arrive at an operator that is essentially the standard two-dimensional Laplacian. Correspondingly, a generalization of the approach from [36] to the Heston model is not directly clear.

Ikonen & Toivanen [26] propose a novel splitting technique, which applies to the Heston LCP obtained after space and time discretization. Their idea, originally put forth in [23] in the case of the Black–Scholes model, is to introduce an auxiliary variable such that a decoupling is achieved between the underlying time discretization scheme and the enforcement of the early exercise constraint. The amount of computational work per time step of this approach is governed by the solution of the pertinent linear systems, for which the authors employ multigrid. The computational cost of the update of the early exercise constraint is negligible. The time discretization

schemes under consideration are backward Euler, Crank–Nicolson and BDF2 as well as a second-order, L -stable Runge–Kutta method. It is shown [25, 26] that this splitting approach performs well and is efficient.

Persson & Von Sydow [31] consider a tailored, adaptive space-time discretization of the Heston PDCP based on finite differences and the BDF2 method and apply the splitting technique from [26] where for the solution of the linear systems a preconditioned GMRES iteration is used.

The main aim of our present paper is to show that by invoking the splitting idea from [26] an effective adaptation of ADI time discretization schemes to the semidiscretized Heston PDCP for American-style options is attained. We refer to the newly obtained methods as ADI-IT methods. The amount of computational work per time step of an ADI-IT method is determined by the solution method for the pertinent linear systems, as in [26]. But, contrary to [26], these linear systems now only involve matrices with a fixed, small bandwidth. They can therefore be exactly and easily solved in an efficient manner by using LU factorization. In our note [13] this approach was already briefly introduced. In the present paper we shall give a comprehensive study. An outline of the rest of the paper is as follows.

Section 2 describes the discretization of the Heston operator (1.1) by finite difference schemes on nonuniform Cartesian grids, leading to a semidiscrete version of the Heston PDCP (1.3). In Section 3, we first consider time discretization by the common θ -method. For the resulting Heston LCP the splitting technique by Ikonen & Toivanen [26] is formulated and discussed. We prove a useful theorem on the closeness of the numerical solutions with and without splitting. Next, in Section 4 our adaptation of ADI time discretization schemes to the semidiscrete Heston PDCP is defined. Four known ADI schemes are considered: the Douglas scheme, the Craig–Sneyd scheme, the modified Craig–Sneyd scheme and the Hundsdorfer–Verwer scheme. Section 5 presents an extensive numerical study of the acquired ADI-IT methods. We investigate in detail their actual stability and convergence behavior in a variety of representative, challenging test cases - with short and long maturity times, with zero and nonzero correlation, for cases where the Feller condition holds and cases where it is violated, and for vanilla American put options as well as capped American put options. Also, approximations obtained with the ADI-IT approach are compared to known approximations from the literature reviewed above and for all test cases the computed option price surfaces and free boundaries are graphically displayed. In Section 6 conclusions are given.

2 Spatial discretization

The first step in numerically solving the Heston PDCP (1.3) is the discretization of the Heston operator (1.1). For the spatial variable s resp. v the domain is restricted to a bounded set $[0, S_{\max}]$ resp. $[0, V_{\max}]$ with fixed values S_{\max} , V_{\max} taken sufficiently large. We deal with boundary conditions of Dirichlet and Neumann type, determined by the specific option under consideration, or no condition, in the case of a degenerate boundary.

For a vanilla American put option the following boundary conditions are common in the literature.

- In the s -direction:

$$u(0, v, t) = K, \tag{2.1a}$$

$$\frac{\partial u}{\partial s}(S_{\max}, v, t) = 0. \tag{2.1b}$$

- In the v -direction:

$$\frac{\partial u}{\partial v}(s, V_{\max}, t) = 0. \tag{2.2}$$

Note the degeneracy feature of the Heston operator (1.1) in the v -direction that all second-order derivative terms vanish and the operator becomes convection-dominated for $v \downarrow 0$. Relatedly, at $v = 0$, it is assumed that the Heston PDCP (1.3) is fulfilled.

For the discretization of (1.1) a suitable Cartesian grid is chosen on $[0, S_{\max}] \times [0, V_{\max}]$ with nonuniform meshes $0 = s_0 < s_1 < \dots < s_{m_1} = S_{\max}$ and $0 = v_0 < v_1 < \dots < v_{m_2} = V_{\max}$ in the s - and v -directions. The use of nonuniform meshes, instead of uniform ones, can substantially improve the efficiency, cf. e.g. [12]. Moreover, when applying the nonuniform meshes defined below, taking larger values for S_{\max} and V_{\max} will be computationally inexpensive.

- In the s -direction: let integer $m_1 \geq 1$ and parameter $d_1 > 0$ and let equidistant points $\xi_{\min} = \xi_0 < \xi_1 < \dots < \xi_{m_1} = \xi_{\max}$ be given with

$$\begin{aligned}\xi_{\min} &= \sinh^{-1} \left(\frac{-S_{\text{left}}}{d_1} \right), \\ \xi_{\text{int}} &= \frac{S_{\text{right}} - S_{\text{left}}}{d_1}, \\ \xi_{\max} &= \xi_{\text{int}} + \sinh^{-1} \left(\frac{S_{\max} - S_{\text{right}}}{d_1} \right).\end{aligned}$$

Note that $\xi_{\min} < 0 < \xi_{\text{int}} < \xi_{\max}$. We then define the mesh $0 = s_0 < s_1 < \dots < s_{m_1} = S_{\max}$ through the transformation

$$s_i = \varphi(\xi_i) \quad (0 \leq i \leq m_1)$$

where

$$\varphi(\xi) = \begin{cases} S_{\text{left}} + d_1 \sinh(\xi) & (\text{for } \xi_{\min} \leq \xi < 0), \\ S_{\text{left}} + d_1 \xi & (\text{for } 0 \leq \xi \leq \xi_{\text{int}}), \\ S_{\text{right}} + d_1 \sinh(\xi - \xi_{\text{int}}) & (\text{for } \xi_{\text{int}} < \xi \leq \xi_{\max}). \end{cases}$$

The above mesh has relatively many points in a given fixed interval $[S_{\text{left}}, S_{\text{right}}] \subset [0, S_{\max}]$. This interval is taken in particular such that it lies in the region of interest in applications and it contains the strike K . Thus numerical difficulties due to the initial function (1.2), which possesses a discontinuous derivative at K , are alleviated. The s -mesh is nonuniform outside $[S_{\text{left}}, S_{\text{right}}]$ and uniform inside.

- In the v -direction: let integer $m_2 \geq 1$ and parameter $d_2 > 0$ and let equidistant points $\psi_0 < \psi_1 < \dots < \psi_{m_2}$ be given by

$$\psi_j = j \cdot \Delta\psi \quad (0 \leq j \leq m_2) \quad \text{with} \quad \Delta\psi = \frac{1}{m_2} \sinh^{-1} \left(\frac{V_{\max}}{d_2} \right).$$

We then define the mesh $0 = v_0 < v_1 < \dots < v_{m_2} = V_{\max}$ by

$$v_j = d_2 \sinh(\psi_j) \quad (0 \leq j \leq m_2).$$

This nonuniform mesh has relatively many points in the neighborhood of the important degenerate boundary $v = 0$.

Let $\Delta\xi = \xi_1 - \xi_0$. It is readily verified that the s - and v -meshes defined above are smooth, in the sense that there exist real constants $C_0, C_1, C_2, C'_0, C'_1, C'_2 > 0$ such that the mesh widths $\Delta s_i = s_i - s_{i-1}$ and $\Delta v_j = v_j - v_{j-1}$ satisfy

$$\begin{aligned}C_0 \Delta\xi \leq \Delta s_i \leq C_1 \Delta\xi & \quad \text{and} \quad |\Delta s_{i+1} - \Delta s_i| \leq C_2 (\Delta\xi)^2 & \quad (\text{uniformly in } i, m_1), \\ C'_0 \Delta\psi \leq \Delta v_j \leq C'_1 \Delta\psi & \quad \text{and} \quad |\Delta v_{j+1} - \Delta v_j| \leq C'_2 (\Delta\psi)^2 & \quad (\text{uniformly in } j, m_2).\end{aligned}$$

The actual choice of parameters in our numerical experiments, in Section 5 below, are $d_1 = K/20$, $d_2 = V_{\max}/500$ and with $r = \frac{1}{4}$,

$$S_{\text{left}} = \max \left(\frac{1}{2}, e^{-rT} \right) K, \quad S_{\text{right}} = K, \quad S_{\max} = 14K, \quad V_{\max} = 5.$$

The above values for S_{\max} , V_{\max} might be considered as large. They were heuristically determined, so as to guarantee that the error induced by the restriction of the spatial domain to a bounded set is negligible in all our experiments. As already mentioned, with the nonuniform meshes under consideration, increasing the upper bounds S_{\max} , V_{\max} is harmless for the overall efficiency. The interval $[S_{\text{left}}, S_{\text{right}}]$ has been chosen such that, in addition to containing the strike K , the s -points of the exercise boundary are expected to be contained in it for all practical values v , t . A further investigation into possibly better parameter values than above may be interesting, but this is beyond the scope of the present paper.

We discuss next the discretization of the spatial derivatives on the selected nonuniform grid. In view of the boundary conditions, given above, the pertinent spatial grid is

$$\mathcal{G} = \{(s_i, v_j) : 1 \leq i \leq m_1, 0 \leq j \leq m_2\}.$$

Write $u_{i,j} = u(s_i, v_j, t)$. We employ the following well-known finite difference (FD) schemes for discretizing the convection and diffusion terms in the Heston operator (1.1).

- In the s -direction:
the *forward scheme for convection*

$$\frac{\partial u}{\partial s}(s_i, v_j, t) \approx \frac{u_{i+1,j} - u_{i,j}}{\Delta s_{i+1}},$$

the *central scheme for diffusion*

$$\frac{\partial^2 u}{\partial s^2}(s_i, v_j, t) \approx \frac{2}{\Delta s_i(\Delta s_i + \Delta s_{i+1})}u_{i-1,j} - \frac{2}{\Delta s_i \Delta s_{i+1}}u_{i,j} + \frac{2}{\Delta s_{i+1}(\Delta s_i + \Delta s_{i+1})}u_{i+1,j}.$$

- In the v -direction:
the *forward scheme for convection*

$$\frac{\partial u}{\partial v}(s_i, v_j, t) \approx \frac{u_{i,j+1} - u_{i,j}}{\Delta v_{j+1}} \quad \text{whenever } v_j \leq \eta,$$

the *backward scheme for convection*

$$\frac{\partial u}{\partial v}(s_i, v_j, t) \approx \frac{u_{i,j} - u_{i,j-1}}{\Delta v_j} \quad \text{whenever } v_j > \eta,$$

the *central scheme for diffusion*

$$\frac{\partial^2 u}{\partial v^2}(s_i, v_j, t) \approx \frac{2}{\Delta v_j(\Delta v_j + \Delta v_{j+1})}u_{i,j-1} - \frac{2}{\Delta v_j \Delta v_{j+1}}u_{i,j} + \frac{2}{\Delta v_{j+1}(\Delta v_j + \Delta v_{j+1})}u_{i,j+1}.$$

For arbitrary meshes the forward and backward FD schemes for convection and central FD scheme for diffusion all possess a first-order truncation error (whenever u is sufficiently often differentiable). For smooth meshes as in our paper, the truncation error of the central scheme is of second-order.

Special attention is needed for the FD discretization at the important degenerate boundary as well as at the boundaries with a Neumann condition.

- In the s -direction: the Neumann condition (2.1b) at $s = S_{\max}$ directly renders the first derivative $\partial u / \partial s$. Using the central scheme, together with linear extrapolation to obtain the required approximation at a virtual mesh point beyond S_{\max} , the second derivative $\partial^2 u / \partial s^2$ is approximated.

- In the v -direction: the Neumann condition (2.2) at $v = V_{\max}$ is treated analogously to (2.1b) above. At the degenerate boundary $v = 0$ we approximate $\partial u / \partial v$ by the forward FD scheme.¹ Next, the term in (1.1) involving $\partial^2 u / \partial v^2$ vanishes if $v = 0$ and is thus trivially dealt with.

If the underlying asset price and variance processes are correlated, so if $\rho \neq 0$, then the Heston operator (1.1) contains a mixed derivative term. For the mixed derivative $\partial^2 u / \partial s \partial v$ we consider a standard FD discretization based on a centered 9-point stencil formed by successive application of the following central FD schemes in the s - and v -directions:

$$\begin{aligned} \frac{\partial u}{\partial s}(s_i, v_j, t) &\approx \frac{-\Delta s_{i+1}}{\Delta s_i(\Delta s_i + \Delta s_{i+1})} u_{i-1,j} + \frac{\Delta s_{i+1} - \Delta s_i}{\Delta s_i \Delta s_{i+1}} u_{i,j} + \frac{\Delta s_i}{\Delta s_{i+1}(\Delta s_i + \Delta s_{i+1})} u_{i+1,j}, \\ \frac{\partial u}{\partial v}(s_i, v_j, t) &\approx \frac{-\Delta v_{j+1}}{\Delta v_j(\Delta v_j + \Delta v_{j+1})} u_{i,j-1} + \frac{\Delta v_{j+1} - \Delta v_j}{\Delta v_j \Delta v_{j+1}} u_{i,j} + \frac{\Delta v_j}{\Delta v_{j+1}(\Delta v_j + \Delta v_{j+1})} u_{i,j+1}. \end{aligned}$$

It is readily verified that at the degenerate boundary as well as the two Neumann boundaries the mixed derivative term in (1.1) vanishes and, hence, is trivially dealt with.

We remark that with the simple first-order FD schemes for convection above, it is easily proved that the obtained semidiscrete Heston matrix A is such that $-A$ is always an M-matrix² if the correlation $\rho = 0$. In the literature on the pricing of financial options, this type of condition has been used for deriving favorable properties of numerical methods. In general, $-A$ is not an M-matrix whenever $\rho \neq 0$ and standard FD discretizations of the mixed derivative, such as above, are applied. More advanced discretizations of the mixed derivative have been constructed in this case, see e.g. [24, 25, 26]. In the present paper we shall adhere to the above standard choice, however.

For an accurate approximation of the option value function u it is beneficial to smoothen the payoff function (1.2) at the strike K , where it is discontinuous in the first derivative. Accordingly, we replace the value of the payoff function at the mesh point s_i nearest to K by its cell average, see e.g. [33]:

$$\frac{1}{h} \int_{s_{i-1/2}}^{s_{i+1/2}} \phi(s) ds \quad \text{with} \quad s_{i-1/2} = \frac{1}{2}(s_{i-1} + s_i), \quad s_{i+1/2} = \frac{1}{2}(s_i + s_{i+1}), \quad h = s_{i+1/2} - s_{i-1/2}.$$

By spatial discretization, the option values $u(s, v, t)$ are approximated at the spatial grid points $(s, v) \in \mathcal{G}$. These approximations form the entries of a vector $U(t)$, which is given as the solution of a *semidiscrete PDCP*,

$$U'(t) \geq AU(t) + g, \quad U(t) \geq U_0, \quad (U(t) - U_0)^T (U'(t) - AU(t) - g) = 0 \quad (0 < t \leq T). \quad (2.3)$$

Here inequalities are to be interpreted componentwise. The size of the system (2.3) equals $M = m_1(m_2 + 1)$, A is a given real $M \times M$ matrix and U_0 and g are given real $M \times 1$ vectors determined by the initial and boundary conditions, respectively. Further, T stands for transpose. The next main step in numerically solving (1.3) is the time discretization of (2.3).

3 Time discretization: θ -method

After the spatial discretization of the Heston PDCP (1.3) in the previous section, we now consider the time discretization of the obtained semidiscrete PDCP (2.3). An often-used scheme for its time discretization is the θ -method, with parameter $\theta \in [\frac{1}{2}, 1]$, see e.g. [7, 21, 24, 25, 26]. The choices $\theta = \frac{1}{2}$ and $\theta = 1$ represent, respectively, the well-known Crank–Nicolson (CN) and backward

¹Some authors deal with the $v = 0$ boundary separately, by applying an explicit time stepping scheme. But this yields an unpractical discretization, where an excessively large number of time steps is necessary for stability.

²For the definition of an M-matrix see e.g. [2].

Euler (BE) methods. These methods have classical orders of consistency equal to two and one, respectively, in the numerical solution of systems of ordinary differential equations (ODEs) and possess favorable linear stability properties, cf. e.g. [14]. Let I denote the $M \times M$ identity matrix, let $\Delta t = T/N$ with integer $N \geq 1$ be a given time step and let temporal grid points $t_n = n \cdot \Delta t$ for integers $0 \leq n \leq N$. Then application of the θ -method to the semidiscrete Heston PDCP (2.3) defines approximations $U_n \approx U(t_n)$ successively for $n = 1, 2, \dots, N$ by

$$(I - \theta \Delta t A)U_n \geq (I + (1 - \theta)\Delta t A)U_{n-1} + \Delta t g, \quad (3.1a)$$

$$U_n \geq U_0, \quad (U_n - U_0)^T ((I - \theta \Delta t A)U_n - (I + (1 - \theta)\Delta t A)U_{n-1} - \Delta t g) = 0. \quad (3.1b)$$

The fully discrete PDCP (3.1) constitutes, for each given n , a so-called *linear complementarity problem (LCP)*. By introducing an auxiliary vector λ_n , it can clearly be rewritten as

$$(I - \theta \Delta t A)U_n = (I + (1 - \theta)\Delta t A)U_{n-1} + \Delta t g + \Delta t \lambda_n, \quad (3.2a)$$

$$\lambda_n \geq 0, \quad U_n \geq U_0, \quad (U_n - U_0)^T \lambda_n = 0. \quad (3.2b)$$

If the i -th component $\lambda_{n,i}$ of λ_n is equal to zero, then the corresponding spatial grid point $(s, v) \in \mathcal{G}$ is assumed to lie in the continuation region at time t_n , and otherwise in the exercise region. We consider in this paper the numerical solution of the LCPs (3.2) for $1 \leq n \leq N$ by employing a splitting technique proposed by Ikonen & Toivanen [23, 26]:

$$(I - \theta \Delta t A)\bar{U}_n = (I + (1 - \theta)\Delta t A)\hat{U}_{n-1} + \Delta t g + \Delta t \bar{\lambda}_n, \quad (3.3a)$$

$$\begin{cases} \hat{U}_n - \bar{U}_n - \Delta t (\hat{\lambda}_n - \bar{\lambda}_n) = 0, \\ \hat{\lambda}_n \geq 0, \quad \hat{U}_n \geq U_0, \quad (\hat{U}_n - U_0)^T \hat{\lambda}_n = 0, \end{cases} \quad (3.3b)$$

where $\hat{U}_0 = U_0$. The vector $\bar{\lambda}_n$ is given at the start of each time step. Here the basic choice from [23, 26] is taken:

$$\bar{\lambda}_n = \hat{\lambda}_{n-1} \quad \text{with } \hat{\lambda}_0 \text{ the zero vector.} \quad (3.4)$$

We refer to the above technique as *Ikonen-Toivanen (IT) splitting* and call (3.3) the θ -IT method. Special cases are the *CN-IT method* and *BE-IT method* given by $\theta = \frac{1}{2}$ and $\theta = 1$, respectively. The IT splitting approach has been inspired by similar techniques in computational fluid dynamics [10]. The vectors \hat{U}_n and $\hat{\lambda}_n$ defined by (3.3) constitute approximations to U_n and λ_n defined by (3.2). These vectors are computed in two, successive stages. In the first stage, an intermediate approximation \bar{U}_n is determined by solving the system of linear equations (3.3a). Notice that this system can be viewed as obtained from application of the classical θ -method to a system of ODEs. In the second stage, \bar{U}_n and $\bar{\lambda}_n$ are updated to \hat{U}_n and $\hat{\lambda}_n$ through (3.3b). It is readily verified that these updates are given by the simple, explicit formulas

$$\hat{U}_n = \max \{ \bar{U}_n - \Delta t \bar{\lambda}_n, U_0 \}, \quad \hat{\lambda}_n = \max \{ 0, \bar{\lambda}_n + (U_0 - \bar{U}_n)/\Delta t \}. \quad (3.5)$$

Here the maximum of two vectors is taken componentwise.

The following useful theorem concerns the difference between the LCP (3.2) and its approximate version (3.3) obtained by IT splitting if $\theta = 1$. For any given diagonal matrix $D \in \mathbb{R}^{M \times M}$ with positive diagonal entries, let the scaled inner product be given by

$$\langle x, y \rangle_D = y^T D x \quad \text{whenever } x, y \in \mathbb{R}^M$$

and let $\| \cdot \|_D$ denote both the induced vector and matrix norms. We have

Theorem 3.1 Consider the processes (3.2) and (3.3) with $\theta = 1$. Assume there exists a positive diagonal matrix D such that

$$DA + A^T D \text{ is negative semidefinite} \quad (3.6)$$

and assume there is a real constant ν independent of $\Delta t > 0$ such that

$$\|\lambda_1\|_D + \sum_{n=2}^N \|\lambda_n - \lambda_{n-1}\|_D \leq \nu. \quad (3.7)$$

Then

$$\max_{1 \leq n \leq N} \|U_n - \widehat{U}_n\|_D \leq \nu \Delta t \quad (3.8)$$

whenever $\Delta t = T/N$, integer $N \geq 1$.

Proof (i) From assumption (3.6) and Berman & Plemmons [2, Chs. 6, 10] it first follows that $Q = I - \Delta t A$ is a P-matrix³ and that (3.1) always possesses a unique solution U_n . By (3.2a),

$$QU_n = U_{n-1} + \Delta t g + \Delta t \lambda_n.$$

By (3.3b),

$$\bar{U}_n = \widehat{U}_n - \Delta t (\widehat{\lambda}_n - \bar{\lambda}_n)$$

and inserting this into (3.3a) yields

$$Q\widehat{U}_n = \widehat{U}_{n-1} + \Delta t g + \Delta t \bar{\lambda}_n + \Delta t Q(\widehat{\lambda}_n - \bar{\lambda}_n).$$

Define $V_n = U_n - \widehat{U}_n$. Then, with $R = Q^{-1}$,

$$QV_n = V_{n-1} + \Delta t (\lambda_n - \bar{\lambda}_n) - \Delta t Q(\widehat{\lambda}_n - \bar{\lambda}_n),$$

$$V_n = RV_{n-1} + \Delta t R(\lambda_n - \bar{\lambda}_n) - \Delta t (\widehat{\lambda}_n - \bar{\lambda}_n).$$

Define $W_n = \Delta t (\lambda_n - \widehat{\lambda}_n)$. Upon writing $\widehat{\lambda}_n - \bar{\lambda}_n = \widehat{\lambda}_n - \lambda_n + \lambda_n - \bar{\lambda}_n$ there follows

$$V_n - W_n = RV_{n-1} + \Delta t S(\lambda_n - \bar{\lambda}_n),$$

with $S = R - I$. Inserting the choice (3.4) for $\bar{\lambda}_n$ leads to

$$V_n - W_n = RV_{n-1} + SW_{n-1} + \Delta t S(\lambda_n - \lambda_{n-1}), \quad (3.9)$$

where we put $\lambda_0 = 0$.

(ii) Conditions (3.2b) and (3.3b) imply for the components of the vectors V_n, W_n that

$$V_{n,i} W_{n,i} \leq 0 \quad \text{for all } i. \quad (3.10)$$

To see this, consider four cases:

If $\lambda_{n,i} = 0$ and $\widehat{\lambda}_{n,i} = 0$, then $W_{n,i} = 0$.

If $\lambda_{n,i} > 0$ and $\widehat{\lambda}_{n,i} = 0$, then $W_{n,i} > 0$ and $V_{n,i} = U_{0,i} - \widehat{U}_{n,i} \leq 0$.

If $\lambda_{n,i} = 0$ and $\widehat{\lambda}_{n,i} > 0$, then $W_{n,i} < 0$ and $V_{n,i} = U_{n,i} - U_{0,i} \geq 0$.

If $\lambda_{n,i} > 0$ and $\widehat{\lambda}_{n,i} > 0$, then $V_{n,i} = U_{0,i} - U_{0,i} = 0$.

³A square matrix is called a P-matrix if all its principal minors are positive, see e.g. [2, 21].

(iii) Define on \mathbb{R}^{2M} the norm

$$\left\| \begin{pmatrix} x \\ y \end{pmatrix} \right\|_D = \sqrt{\|x\|_D^2 + \|y\|_D^2} \quad \text{whenever } x, y \in \mathbb{R}^M$$

with induced matrix norm denoted the same. By (3.10), we have

$$\left\| \begin{pmatrix} V_n \\ W_n \end{pmatrix} \right\|_D^2 = \|V_n\|_D^2 + \|W_n\|_D^2 \leq \|V_n\|_D^2 + \|W_n\|_D^2 - 2\langle V_n, W_n \rangle_D = \|V_n - W_n\|_D^2.$$

Using (3.9) this yields

$$\left\| \begin{pmatrix} V_n \\ W_n \end{pmatrix} \right\|_D \leq \left\| \begin{pmatrix} R & S \\ O & O \end{pmatrix} \begin{pmatrix} V_{n-1} \\ W_{n-1} \end{pmatrix} \right\|_D + \Delta t \|S(\lambda_n - \lambda_{n-1})\|_D. \quad (3.11)$$

Consider the 2×2 matrix-valued rational function Φ given by

$$\Phi(z) = \begin{pmatrix} \frac{1}{1-z} & \frac{z}{1-z} \\ 0 & 0 \end{pmatrix}$$

for $z \in \mathbb{C}$. Then

$$\Phi(\Delta t A) = \begin{pmatrix} R & S \\ O & O \end{pmatrix}.$$

For the spectral norm of $\Phi(z)$ it is easily shown that

$$\|\Phi(z)\|_2^2 = \lambda_{\max}[\Phi(z)^* \Phi(z)] = \frac{1 + |z|^2}{|1 - z|^2},$$

which yields

$$\|\Phi(z)\|_2 \leq 1 \quad \text{if and only if } \Re z \leq 0. \quad (3.12)$$

Next, the condition (3.6) on matrix A is equivalent to

$$\Re \langle Ax, x \rangle_D \leq 0 \quad \text{whenever } x \in \mathbb{C}^M, \quad (3.13)$$

where $\langle x, y \rangle_D = y^* D x$ for any given vectors $x, y \in \mathbb{C}^M$. In view of (3.12) and (3.13), we can invoke a matrix-valued version of a well-known theorem due to von Neumann, see e.g. [14, Sect. V.7]. This directly leads to

$$\|\Phi(\Delta t A)\|_D \leq 1.$$

By (3.11), it thus follows that

$$\left\| \begin{pmatrix} V_n \\ W_n \end{pmatrix} \right\|_D \leq \left\| \begin{pmatrix} V_{n-1} \\ W_{n-1} \end{pmatrix} \right\|_D + \Delta t \|\lambda_n - \lambda_{n-1}\|_D \leq \dots \leq \Delta t \sum_{j=1}^n \|\lambda_j - \lambda_{j-1}\|_D \leq \nu \Delta t,$$

which completes the proof. □

Theorem 3.1 provides the useful result that the sequence $\{\widehat{U}_n\}$ generated by (3.3) is $\mathcal{O}(\Delta t)$ close to the sequence $\{U_n\}$ defined by (3.2) if $\theta = 1$. Observe that there is no restriction on the time step Δt .

The matrix condition (3.6), or the equivalent condition (3.13), are well-known. In the numerical ODE literature they are often referred to by saying that a scaled logarithmic 2-norm of A is less than or equal to zero. Recently In 't Hout & Volders [18] investigated this condition in the case of the Heston PDE. Even though the FD discretization studied in there differs somewhat from the one considered here, it is interesting to note that a positive result concerning (3.13) was proved

[18] for arbitrary correlation factors $\rho \in [-1, 1]$ with a natural scaling matrix D . The extension of this (nontrivial) result to the present semidiscretization will be left as a topic for future research.

The condition (3.7), on the λ_n defined by (3.2), is analogous to a condition by Ikonen & Toivanen [26], except that these authors dealt with the maximum norm. Theoretical and numerical evidence indicates that a moderate constant ν exists that is valid uniformly in the spatial grid and the time step such that (3.7) is fulfilled.

Theorem 3.1 is closely related to [26, Thm. 1]. The latter theorem provides an upper bound on the maximum norm of $U_n - \widehat{U}_n$ if $\theta = \frac{1}{2}$. Unfortunately, however, the derivation of this result is not clear as the last statement in the proof of [26, Lemma 2] does not hold in general. Also, a restriction on the time step has been assumed that is often too severe for practical applications.

An analogue of Theorem 3.1 for the important case of the maximum norm is not obvious. Note that our proof above relies in an essential way on the use of inner product norms. Nevertheless, in the numerical experiments below we shall always deal with the maximum norm.

Theorem 3.1 can be extended, along the same line of proof above, to any given parameter value $\theta \in [0, 1)$ if the condition (3.6) is replaced by

$$\|\Delta t A + \gamma I\|_D \leq \gamma \quad \text{with} \quad \gamma = (1 - \theta)^{-2}.$$

This is often called a circle condition on $\Delta t A$. It is substantially stronger than (3.6). In particular it implies that $\|\Delta t A\|_D \leq 2\gamma$, which yields an upper bound on the time step that is often too severe in practice. In the numerical experiments below however, we shall consider the θ -IT method (3.3) both with $\theta = 1$ and $\theta = \frac{1}{2}$.

4 Time discretization: ADI schemes

When numerically solving multidimensional problems, the spatial discretization rapidly leads to very large systems of semidiscrete PDCPs. Applying the θ -IT method then renders very large linear systems with a large bandwidth that need to be solved. This can be computationally very demanding. One good possibility is to employ tailored multigrid methods, as is done e.g. in [26]. In the present paper we propose to combine ADI time discretization schemes with the IT splitting approach for solving (2.3). In (3.3) the θ -method is thus replaced with an ADI scheme.

We shall consider four different schemes of the ADI type: the Douglas scheme (Do), the Craig–Sneyd scheme (CS), the modified Craig–Sneyd scheme (MCS) and the Hundsdorfer–Verwer scheme (HV). These four schemes have recently been elaborately investigated in the numerical pricing of European-style vanilla and barrier options under the Heston model [16] as well as under the three-dimensional Heston–Hull–White and Heston–Cox–Ingersoll–Ross models, see [12] and [11], respectively. It was found that in particular the MCS and HV schemes, with a proper choice of their parameter, are highly efficient, stable and robust. A first brief numerical study of ADI schemes adapted to the pricing of American-style options under the Heston model was carried out in [13]. In this paper we shall substantially extend the promising initial results obtained in loc. cit.

When considering schemes of the ADI type, the semidiscrete matrix A is split into several convenient parts. In the case of the Heston model we have

$$A = A_0 + A_1 + A_2.$$

Here the matrix A_0 is the part of A that stems from the FD discretization of the mixed derivative term and A_1 and A_2 are given by the parts of A that correspond to the FD discretization of all spatial derivatives in the s - and v -directions, respectively, and further contain an equal part of the ru term from (1.1). Note that the matrices A_1 and A_2 are essentially tridiagonal and that the matrix A_0 is nonzero whenever the correlation ρ is nonzero.

Let $\theta > 0$ be a given real parameter. Let $\Delta t = T/N$ with integer $N \geq 1$ and set $t_n = n \Delta t$. The following four methods are given by combination of the ADI schemes mentioned above with the IT splitting stage (3.3b), or equivalently, (3.5). Each method defines successive approximations \widehat{U}_n to the solution vectors $U(t_n)$ of (2.3) for $n = 1, 2, \dots, N$. We refer to them as *ADI-IT methods*.

Do-IT:

$$\begin{cases} Y_0 = \widehat{U}_{n-1} + \Delta t(A\widehat{U}_{n-1} + g) + \Delta t \bar{\lambda}_n, \\ Y_j = Y_{j-1} + \theta \Delta t A_j (Y_j - \widehat{U}_{n-1}) \\ \bar{U}_n = Y_2, \end{cases} \quad (j = 1, 2), \quad (4.1)$$

$$\begin{cases} \widehat{U}_n = \max \{ \bar{U}_n - \Delta t \bar{\lambda}_n, U_0 \}, \\ \widehat{\lambda}_n = \max \{ 0, \bar{\lambda}_n + (U_0 - \bar{U}_n)/\Delta t \}. \end{cases}$$

CS-IT:

$$\begin{cases} Y_0 = \widehat{U}_{n-1} + \Delta t(A\widehat{U}_{n-1} + g) + \Delta t \bar{\lambda}_n, \\ Y_j = Y_{j-1} + \theta \Delta t A_j (Y_j - \widehat{U}_{n-1}) \\ \tilde{Y}_0 = Y_0 + \frac{1}{2} \Delta t A_0 (Y_2 - \widehat{U}_{n-1}), \\ \tilde{Y}_j = \tilde{Y}_{j-1} + \theta \Delta t A_j (\tilde{Y}_j - \widehat{U}_{n-1}) \\ \bar{U}_n = \tilde{Y}_2, \end{cases} \quad (j = 1, 2), \quad (4.2)$$

$$\begin{cases} \widehat{U}_n = \max \{ \bar{U}_n - \Delta t \bar{\lambda}_n, U_0 \}, \\ \widehat{\lambda}_n = \max \{ 0, \bar{\lambda}_n + (U_0 - \bar{U}_n)/\Delta t \}. \end{cases}$$

MCS-IT:

$$\begin{cases} Y_0 = \widehat{U}_{n-1} + \Delta t(A\widehat{U}_{n-1} + g) + \Delta t \bar{\lambda}_n, \\ Y_j = Y_{j-1} + \theta \Delta t A_j (Y_j - \widehat{U}_{n-1}) \\ \tilde{Y}_0 = Y_0 + (\theta \Delta t A_0 + (\frac{1}{2} - \theta) \Delta t A) (Y_2 - \widehat{U}_{n-1}), \\ \tilde{Y}_j = \tilde{Y}_{j-1} + \theta \Delta t A_j (\tilde{Y}_j - \widehat{U}_{n-1}) \\ \bar{U}_n = \tilde{Y}_2, \end{cases} \quad (j = 1, 2), \quad (4.3)$$

$$\begin{cases} \widehat{U}_n = \max \{ \bar{U}_n - \Delta t \bar{\lambda}_n, U_0 \}, \\ \widehat{\lambda}_n = \max \{ 0, \bar{\lambda}_n + (U_0 - \bar{U}_n)/\Delta t \}. \end{cases}$$

HV-IT:

$$\begin{cases} Y_0 = \widehat{U}_{n-1} + \Delta t(A\widehat{U}_{n-1} + g) + \Delta t \bar{\lambda}_n, \\ Y_j = Y_{j-1} + \theta \Delta t A_j (Y_j - \widehat{U}_{n-1}) \\ \tilde{Y}_0 = Y_0 + \frac{1}{2} \Delta t A (Y_2 - \widehat{U}_{n-1}), \\ \tilde{Y}_j = \tilde{Y}_{j-1} + \theta \Delta t A_j (\tilde{Y}_j - Y_2) \\ \bar{U}_n = \tilde{Y}_2, \end{cases} \quad (j = 1, 2), \quad (4.4)$$

$$\begin{cases} \widehat{U}_n = \max \{ \bar{U}_n - \Delta t \bar{\lambda}_n, U_0 \}, \\ \widehat{\lambda}_n = \max \{ 0, \bar{\lambda}_n + (U_0 - \bar{U}_n)/\Delta t \}. \end{cases}$$

As in Section 3, the vector $\bar{\lambda}_n$ is given at the start of each time step by the choice (3.4).

The Do-IT method can be viewed as a natural analogue of the θ -IT method: upon formally setting $A_0 = A_2 = 0$ and $A_1 = A$, one recovers (3.3) from (4.1). The CS-IT, MCS-IT, HV-IT methods form different extensions to the Do-IT method. Indeed, their first two lines are identical to those of Do-IT. They require about twice the amount of computational work per time step. Observe that if $A_0 = 0$, then the CS-IT method reduces to the Do-IT method.

For each ADI-IT method, the *underlying ADI scheme* for the ODE system $U'(t) = AU(t) + g$ is given by the first part, defining \bar{U}_n , where one just omits the $\Delta t \bar{\lambda}_n$ term from the first line and replaces \hat{U}_{n-1} and \bar{U}_n by U_{n-1} and U_n , respectively. The above adaptation of the ADI technique from European- to American-style options is thus very simple.

In the underlying ADI schemes, the matrix A_0 is always handled in an explicit fashion, while the matrices A_1 and A_2 are treated in an implicit fashion. Application of each of the four ADI-IT methods (4.1), (4.2), (4.3), (4.4) requires solving linear systems with the two matrices $(I - \theta \Delta t A_j)$ for $j = 1, 2$. Since these matrices are both tridiagonal, the solution can be done very efficiently by computing once, beforehand, their LU factorizations and then use these in all time steps. Thus the computational cost per time step of each ADI-IT method is directly proportional to the number of spatial grid points M , i.e., the same as in the case of European-style options. Note that the computational cost of the second part of each method, the update (3.5), is negligible.

The order of consistency in the nonstiff sense of the underlying ADI schemes is always one for the Do scheme whenever A_0 is nonzero; it is two for the CS scheme provided that $\theta = \frac{1}{2}$ and two for the MCS and HV schemes for any given θ . In the literature substantial attention has recently been given to the study of unconditional von Neumann stability for ADI schemes when applied to multidimensional convection-diffusion equations with mixed spatial derivative terms, cf. [8, 17, 19, 20, 27, 28]. Here positive results were proved, guaranteeing unconditional stability on various convection-diffusion problem classes under sharp lower bounds on the parameter θ of each ADI scheme. Based on the obtained stability results for two-dimensional problems with mixed derivative term, we select the following values of θ :

- the Do-IT method: $\theta = \frac{1}{2}$
- the CS-IT method: $\theta = \frac{1}{2}$
- the MCS-IT method: $\theta = \frac{1}{3}$
- the HV-IT method: $\theta = \frac{1}{2} + \frac{1}{6}\sqrt{3}$.

At present a rigorous theoretical stability and convergence analysis of ADI-IT methods for semidiscrete PDCPs is beyond reach. In the following section we carry out an extensive numerical investigation. We shall study the four methods selected above, in the application to a variety of representative, challenging Heston test cases.

5 Numerical experiments

For the θ -IT and ADI-IT methods define the *global temporal discretization error* by

$$\hat{e}(\Delta t; m_1, m_2) = \max\{|U_l(T) - \hat{U}_{N,l}| : (s_i, v_j) \in ROI\}. \quad (5.1)$$

Here $U(T)$ represents the exact solution to the semidiscrete Heston PDCP (2.3) at time T and

$$ROI = (\frac{1}{2}K, \frac{3}{2}K) \times (0, 1)$$

is a natural region of interest. The index l in the above is such that the l -th component of a vector corresponds to the spatial grid point (s_i, v_j) . Clearly, (5.1) represents a maximum norm on the ROI .

In this section we numerically investigate the actual behavior of the global temporal errors as a function of Δt for the four ADI-IT methods selected at the end of Section 4. Along with this, the BE-IT and CN-IT methods from Section 3 are briefly considered. For the numerical

experiments we choose six cases of parameter sets, listed in Table 1. The cases A, B, C stem from [3, 32, 38], respectively. Here the Feller condition is always satisfied. The cases D, E, F all stem from [1]. Here the Feller condition is always strongly violated and, in addition, the maturity times are relatively long. The six test cases of Table 1 have, all or in part, been recently considered in the numerical PDE pricing of European options under the Heston model in [16], under the Heston–Hull–White model in [12] and under the Heston–Cox–Ingersoll–Ross model in [11].

	Case A	Case B	Case C	Case D	Case E	Case F
κ	3	0.6067	2.5	0.5	0.3	1
η	0.12	0.0707	0.06	0.04	0.04	0.09
σ	0.04	0.2928	0.5	1	0.9	1
ρ	0.6 (0)	-0.7571 (0)	-0.1 (0)	-0.9 (0)	-0.5 (0)	-0.3 (0)
r	0.01	0.03	0.0507	0.05	0.04	0.03
T	1	3	0.25	10	15	5
K	100	100	100	100	100	100

Table 1: Parameter sets for the Heston model and American put options

Numerical experience has shown that, for efficiency, one can use much less spatial grid points in the v -direction than in the s -direction. Accordingly, we always set

$$m_1 = 2m_2 = 2m.$$

Since a closed-form analytic solution to the semidiscrete Heston PDCP (2.3) is not at hand, we computed in each case a reference solution for $U(T)$ by applying either the CN-IT method or the MCS-IT method using $N = 20\,000$ time steps.

In the following we first consider vanilla American put options. The global temporal errors (5.1) are studied in detail for the six methods under consideration in all six cases of Table 1. We then compare American put option price approximations given in the literature to approximations computed using the ADI-IT technique. Next, for all cases A–F, the obtained option price surfaces and free boundaries are displayed. We conclude the section with experiments for a more exotic American-style option, the capped American put.

For vanilla American put options, Figure 1 displays for the Do-IT, CS-IT, MCS-IT, HV-IT methods as well as the BE-IT and CN-IT methods the global temporal errors $\hat{e}(\Delta t; 2m, m)$ versus Δt in all cases A–F with $\rho = 0$ for a sequence of 20 step sizes $10^{-3} \leq \Delta t \leq 10^0$ with $m = 50$. Note that the results for Do-IT and CS-IT are the same in this experiment, since $A_0 = 0$.

As a first main observation, for each method the temporal errors all remain below a moderate value in each case, and further, they decrease monotonically as Δt decreases. This indicates an unconditionally stable behavior of each method, which is a favorable and nontrivial result.

Concerning the actual convergence behavior, it is readily seen from Figure 1 that the temporal errors as a function of Δt are bounded from above in each case by $C(\Delta t)^p$ with some moderate constant C where $p \approx 1$ for the BE-IT method and $p \approx 2$ for the MCS-IT and HV-IT methods. The observed orders of convergence p for these three methods thus agree with the classical (nonstiff) orders of consistency of their underlying time-discretization schemes for ODEs. This constitutes a second positive and nontrivial result.

In all cases A–F for the CN-IT method and in the cases A–C for the Do-IT and CS-IT methods, one observes in Figure 1 relatively large temporal errors for moderate values of Δt , compared to what one may expect based on their error behavior for small Δt . This undesirable phenomenon is related to the nonsmoothness of the initial (payoff) function. It is already well-known in the literature and as a remedy it is common to apply backward Euler damping, also called Rannacher time stepping. In line with this damping procedure, we consider taking first two BE-IT substeps with $\Delta t/2$ at $t = 0$ and then proceed onwards from $t = \Delta t$ with the method under consideration.

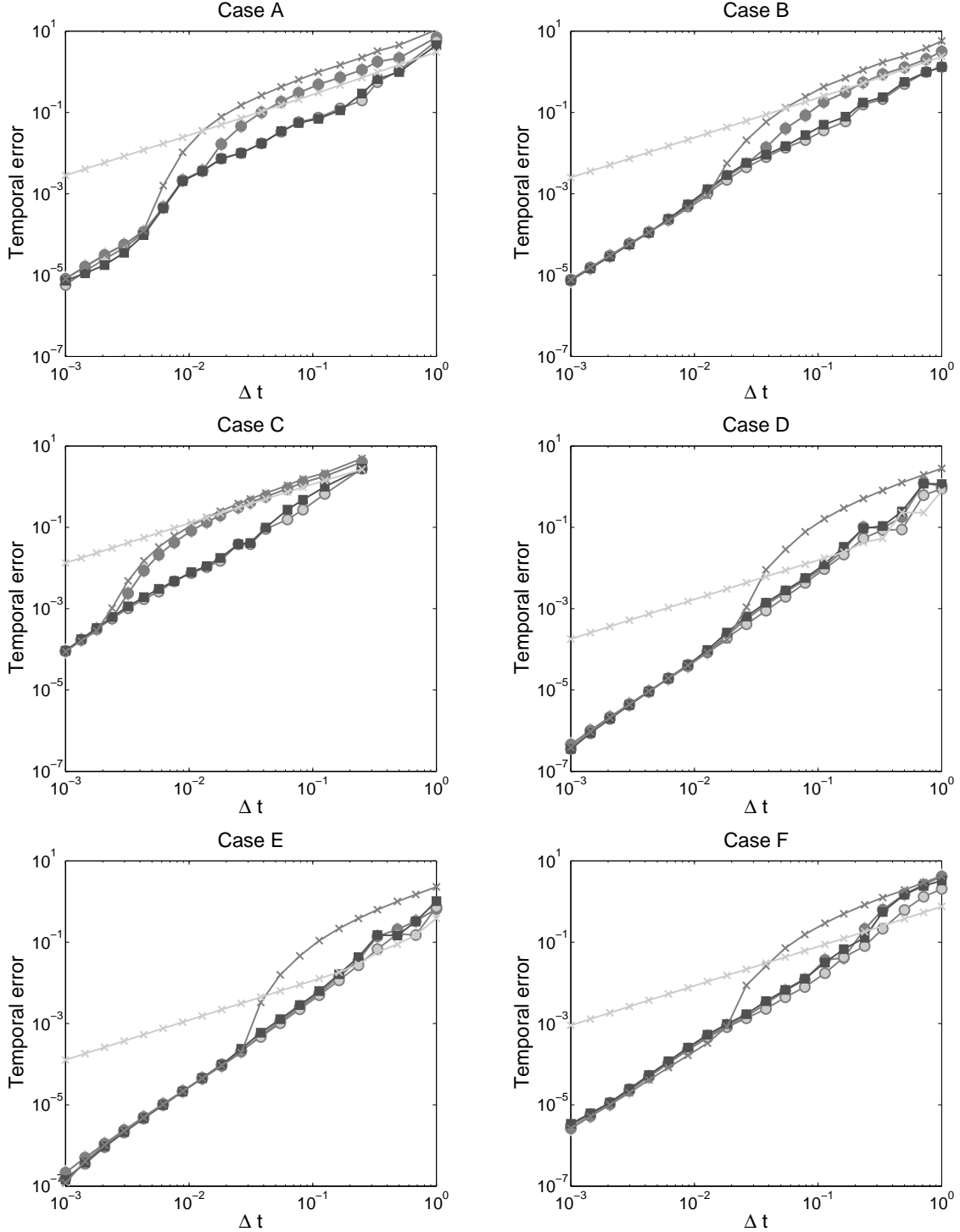


Figure 1: Temporal errors $\hat{e}(\Delta t; 100, 50)$ vs. Δt for vanilla American put options in the six cases of Table 1 with $\rho = 0$ and reference solution by CN-IT with $N = 20\,000$. Two θ -IT methods: BE-IT (light x), CN-IT (dark x). Four ADI-IT methods: Do-IT with $\theta = \frac{1}{2}$ (light diamond), CS-IT with $\theta = \frac{1}{2}$ (dark circle), MCS-IT with $\theta = \frac{1}{3}$ (light circle) and HV-IT with $\theta = \frac{1}{2} + \frac{1}{6}\sqrt{3}$ (dark square). No damping applied.

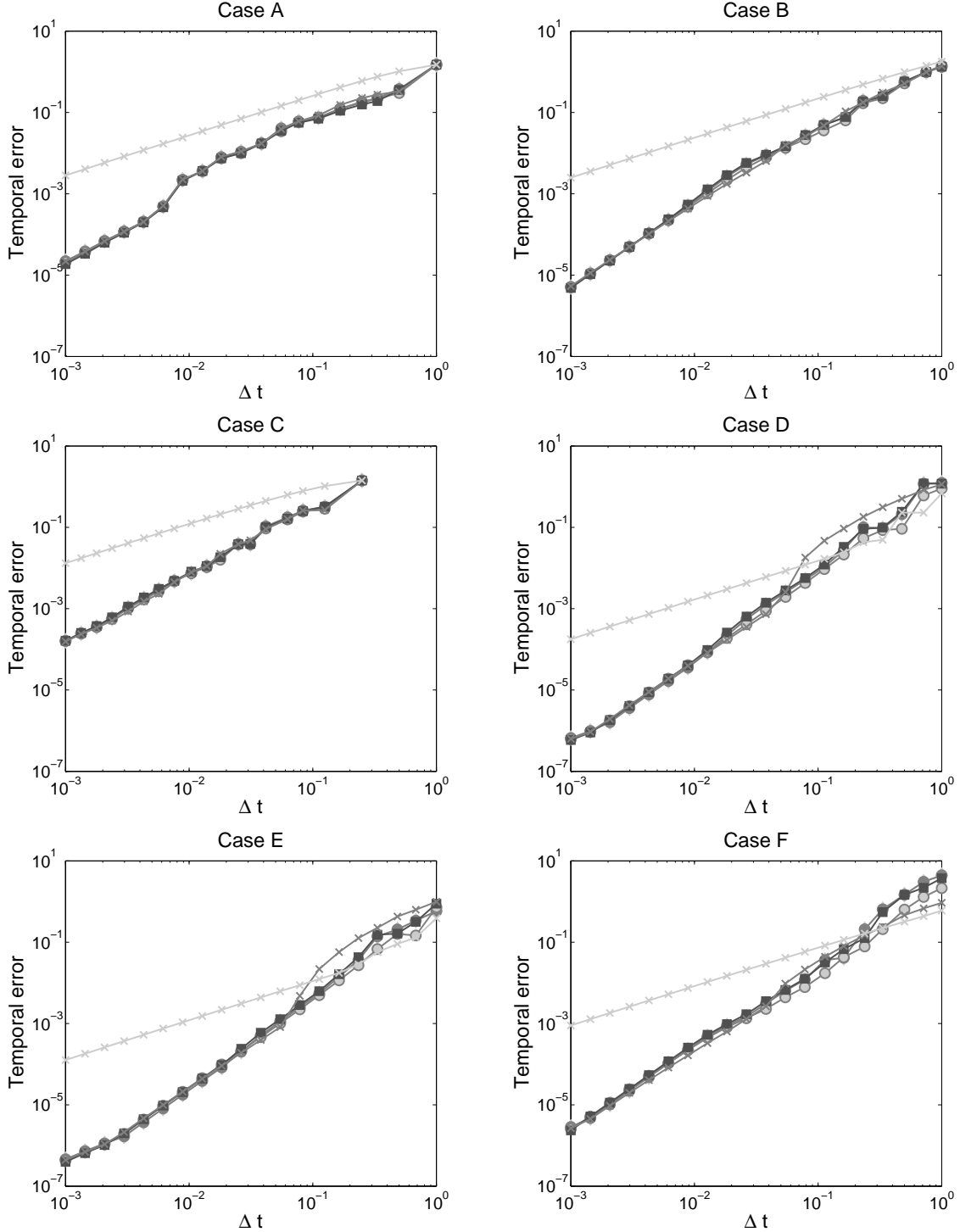


Figure 2: Temporal errors $\hat{e}(\Delta t; 100, 50)$ vs. Δt for vanilla American put options in the six cases of Table 1 with $\rho = 0$ and reference solution by CN-IT with $N = 20\,000$. Two θ -IT methods: BE-IT (light x), CN-IT (dark x). Four ADI-IT methods: Do-IT with $\theta = \frac{1}{2}$ (light diamond), CS-IT with $\theta = \frac{1}{2}$ (dark circle), MCS-IT with $\theta = \frac{1}{3}$ (light circle) and HV-IT with $\theta = \frac{1}{2} + \frac{1}{6}\sqrt{3}$ (dark square). All methods with damping - two steps $\Delta t/2$ with BE-IT.

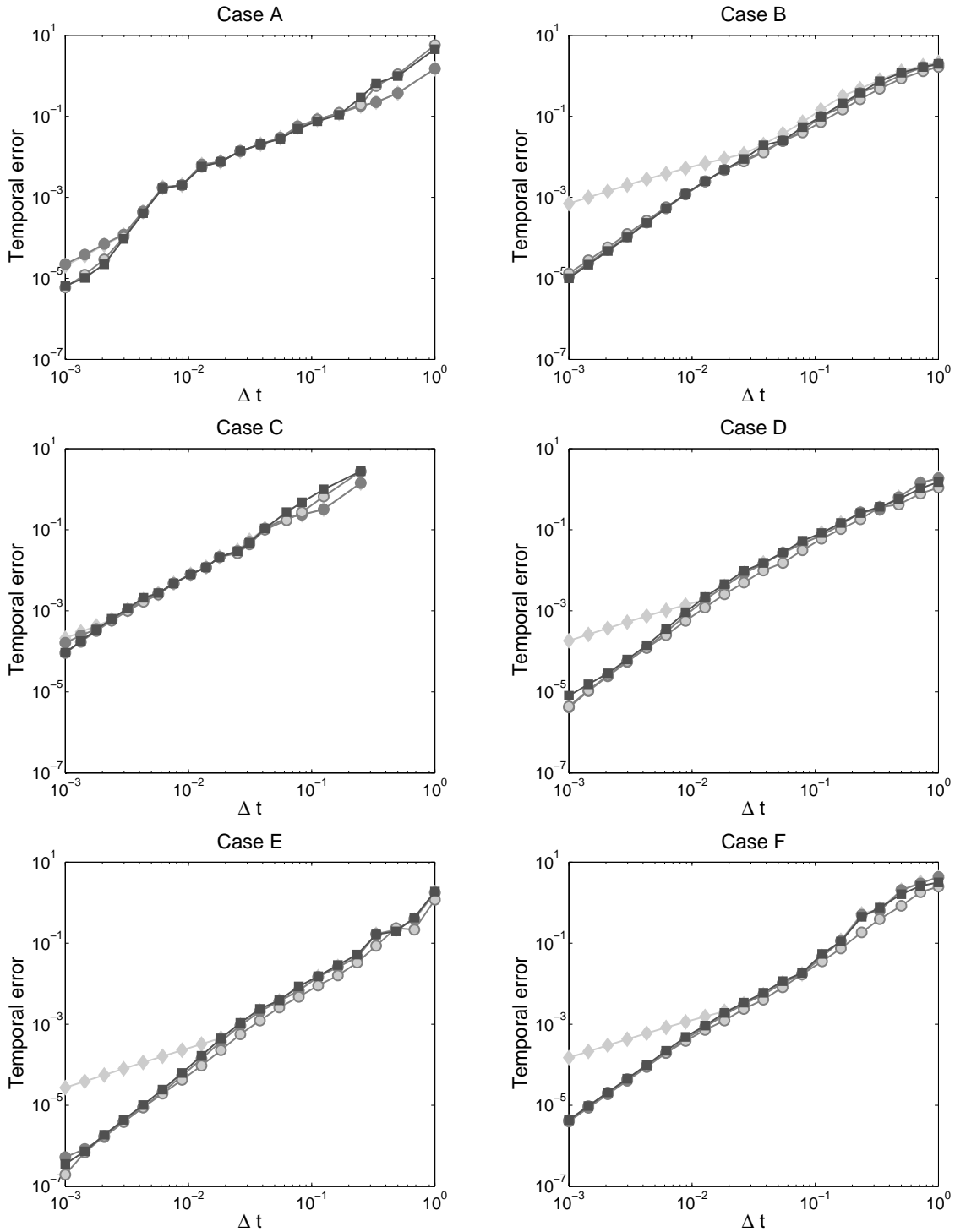


Figure 3: Temporal errors $\hat{e}(\Delta t; 100, 50)$ vs. Δt for vanilla American put options in the six cases in Table 1 with $\rho \neq 0$ and reference solution by MCS-IT with $N = 20\,000$. Four ADI-IT methods: Do-IT with $\theta = \frac{1}{2}$ (light diamond), CS-IT with $\theta = \frac{1}{2}$ (dark circle), MCS-IT with $\theta = \frac{1}{3}$ (light circle) and HV-IT with $\theta = \frac{1}{2} + \frac{1}{6}\sqrt{3}$ (dark square). Do-IT and CS-IT with damping - two steps $\Delta t/2$ with BE-IT.

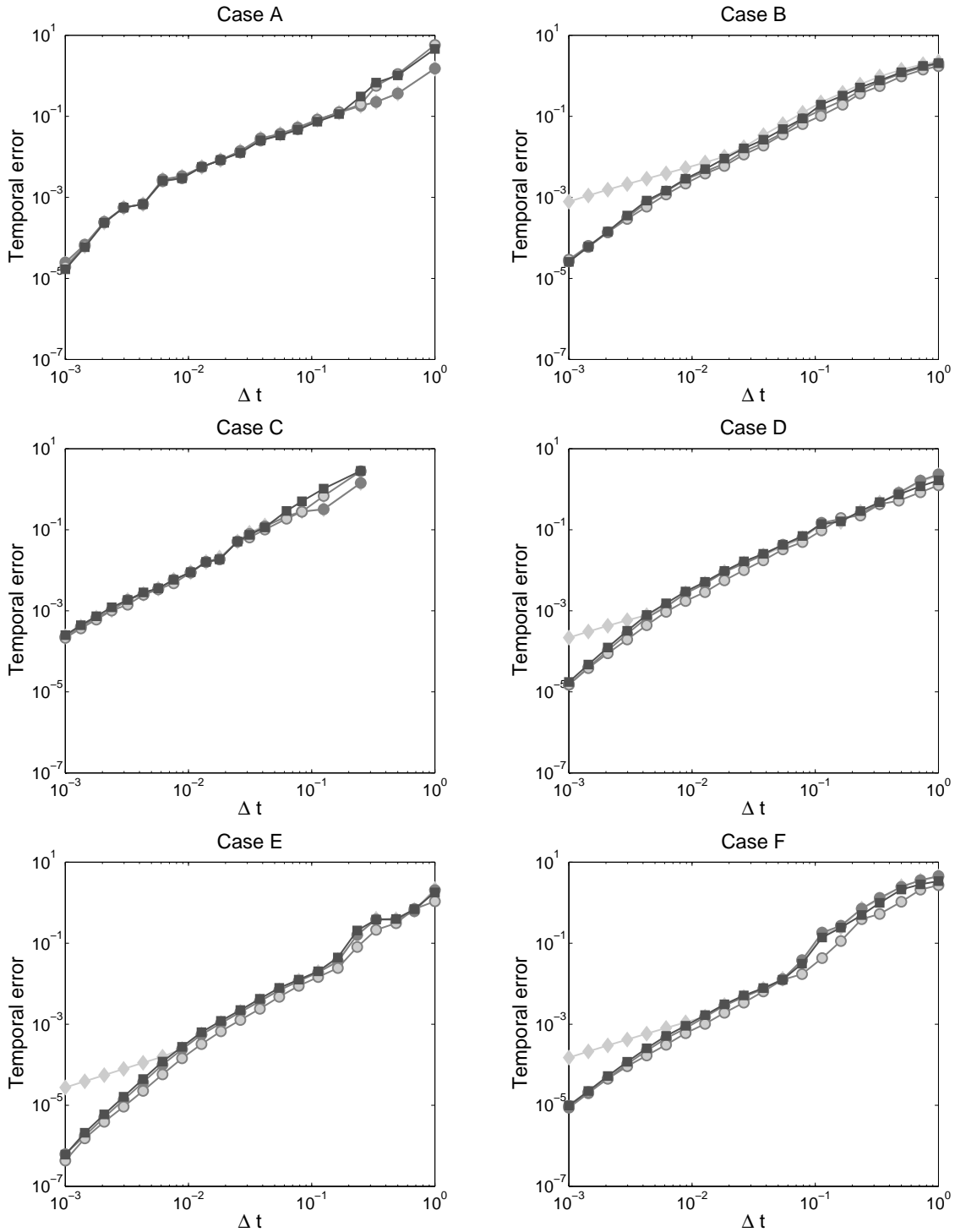


Figure 4: Temporal errors $\hat{e}(\Delta t; 200, 100)$ vs. Δt for vanilla American put options in the six cases in Table 1 with $\rho \neq 0$ and reference solution by MCS-IT with $N = 20\,000$. Four ADI-IT methods: Do-IT with $\theta = \frac{1}{2}$ (light diamond), CS-IT with $\theta = \frac{1}{2}$ (dark circle), MCS-IT with $\theta = \frac{1}{3}$ (light circle) and HV-IT with $\theta = \frac{1}{2} + \frac{1}{6}\sqrt{3}$ (dark square). Do-IT and CS-IT with damping - two steps $\Delta t/2$ with BE-IT.

The result, for all six methods in all six cases, is displayed in Figure 2. Clearly the undesirable phenomenon for the CN-IT, Do-IT and CS-IT methods is mitigated, and for each Δt their temporal errors are now almost the same as for the MCS-IT and HV-IT methods.

A careful inspection of case C in Figure 2 shows a convergence order that is slightly smaller than 2, namely about 1.7, for all methods (except BE-IT which has only order 1). The difference between convergence orders 2 and 1.7 is not readily visible in a figure and the significance of the observation is not completely clear to us. A possible explanation may lie in the short maturity time and corresponding nonsmoothness of the option pricing function in this case. We note that the lower order in case C did not improve by using the variable time step strategy from [26].

In the subsequent experiments we focus on the ADI-IT methods. Here, in view of the above, the Do-IT and CS-IT methods are applied with the BE-IT damping procedure. Thus we consider:

- the Do-IT method with $\theta = \frac{1}{2}$ and damping
- the CS-IT method with $\theta = \frac{1}{2}$ and damping
- the MCS-IT method with $\theta = \frac{1}{3}$
- the HV-IT method with $\theta = \frac{1}{2} + \frac{1}{6}\sqrt{3}$.

Figure 3 displays for these four methods the global temporal errors $\hat{e}(\Delta t; 100, 50)$ versus Δt in all cases A–F, now with correlation $\rho \neq 0$. The figure demonstrates that also with nonzero correlation all ADI-IT methods show an unconditionally stable behavior. For the CS-IT, MCS-IT and HV-IT methods, the temporal errors are bounded from above by $C(\Delta t)^p$ with $p \approx 2$, except in case C where again $p \approx 1.7$. The Do-IT method often has temporal errors that are almost the same as for the latter three methods. A further investigation reveals that the regions of time steps where this occurs are precisely those where Do-IT possesses large temporal errors if no damping would have been applied. Once Δt gets sufficiently small, then a first-order convergence behavior for this method sets in, as expected. We note that in cases A, C this is not observed in the figure; here it happens for $\Delta t < 10^{-3}$.

To gain insight into the dependence of the temporal convergence behavior on the number of spatial grid points M , we have doubled the number of mesh points the s - and v -directions. Figure 4 displays the obtain errors $\hat{e}(\Delta t; 200, 100)$ versus Δt . Comparing with Figure 3 we see that the temporal errors are at most mildly affected by the strong increase in M . This suggests that the convergence behavior of the four ADI-IT methods is valid in the so-called stiff sense, which forms a key property of effective time discretization methods.

The implementation of all methods has been done in Matlab where all matrices have been defined as sparse. As an indication for the CPU times, the CS-IT, MCS-IT and HV-IT methods each took about 0.003, 0.01, 0.02 seconds per time step if $m = 50, 100, 150$, respectively, on one Intel Core Duo T7250 2.00 GHz processor with 4 GB memory. For the Do-IT method these times are about halved.

We next validate the American option pricing method from this paper by comparing its results with approximations already given in the literature. The MCS-IT method is chosen as a representative from the ADI-IT class. To test the numerical valuation of American put options in the Heston model, many authors have considered the parameter set

$$\kappa = 5, \quad \eta = 0.16, \quad \sigma = 0.9, \quad \rho = 0.1, \quad r = 0.1, \quad T = 0.25, \quad K = 10, \quad (5.2)$$

with spot asset prices and variances given by $s = S_0 \in \{8, 9, 10, 11, 12\}$ and $v = V_0 \in \{0.0625, 0.25\}$. We approximated the pertinent (unknown) exact option prices by FD discretization with $m = 50, 100, 150$ and applying the MCS-IT method with $N = 25, 50, 75$ time steps, respectively. Next spline interpolation was used to compute approximations at the off-grid points $(s, v) = (S_0, V_0)$. Our results are given in the upper part of Tables 2 (for $V_0 = 0.0625$) and 3 (for $V_0 = 0.25$). In the lower part, the two tables show approximations obtained by Zvan, Forsyth & Vetzal [39, Table 2], Ikonen & Toivanen [26, Table 1], Persson & Von Sydow [31, Tables 2, 3], Oosterlee [29, Table 5.2], Clarke & Parrott [6] and Vellekoop & Nieuwenhuis [35, Table 4]. The latter paper

employs tree-based methods. The reference prices taken from [26] were computed using a second-order, L -stable Runge–Kutta (RK) scheme in the IT splitting approach. Tables 2 and 3 show that our option prices are nicely in line with those obtained, by different discretization techniques, in the literature.

	m_1	m_2	N	8	9	10	11	12
MCS-IT	100	50	25	2.0001	1.1088	0.5209	0.2152	0.0836
	200	100	50	2.0000	1.1083	0.5206	0.2146	0.0830
	300	150	75	2.0000	1.1081	0.5204	0.2143	0.0827
[39] ZFV	177	103		2.0000	1.1076	0.5202	0.2138	0.0821
[26] RK-IT	320	128	64	2.0000	1.1076	0.5199	0.2135	0.0820
[31] PS	81	21	329	1.9998	1.1085	0.5195	0.2150	0.0822
[29] O	256	256		2.00	1.107	0.517	0.212	0.0815
[6] CP				2.0000	1.1080	0.5316	0.2261	0.0907
[35] VN	1000	48	71	1.9968	1.1076	0.5202	0.2134	0.0815

Table 2: Vanilla American put prices for parameter set (5.2), $S_0 \in \{8, 9, 10, 11, 12\}$, $V_0 = 0.0625$. Upper part: approximations using MCS-IT method with $\theta = \frac{1}{3}$. Lower part: approximations from the literature.

	m_1	m_2	N	8	9	10	11	12
MCS-IT	100	50	25	2.0793	1.3342	0.7963	0.4488	0.2438
	200	100	50	2.0789	1.3340	0.7963	0.4487	0.2435
	300	150	75	2.0788	1.3339	0.7962	0.4486	0.2433
[39] ZFV	177	103		2.0784	1.3337	0.7961	0.4483	0.2428
[26] RK-IT	320	128	64	2.0785	1.3336	0.7959	0.4482	0.2427
[31] PS	81	21	329	2.0784	1.3333	0.7955	0.4479	0.2426
[29] O	256	256		2.079	1.334	0.796	0.449	0.243
[6] CP				2.0733	1.3290	0.7992	0.4536	0.2502

Table 3: Vanilla American put prices for parameter set (5.2), $S_0 \in \{8, 9, 10, 11, 12\}$, $V_0 = 0.25$. Upper part: approximations using MCS-IT method with $\theta = \frac{1}{3}$. Lower part: approximations from the literature.

For the parameter set (5.2) the Feller condition is satisfied. A test set where Feller is violated, and reference prices for American put options are given, is not included in the references above. We choose here a parameter set that has recently been considered by Fang & Oosterlee [9] in the numerical pricing of Bermudan options under the Heston model, where the Feller condition does not hold:

$$\kappa = 1.15, \eta = 0.0348, \sigma = 0.39, \rho = -0.64, r = 0.04, T = 0.25, K = 100, \quad (5.3)$$

with spot asset prices and variance given by $s = S_0 \in \{90, 100, 110\}$ and $v = V_0 = 0.0348$. The upper part of Table 4 displays the pertinent Bermudan put option prices approximated by the COS method from [9, Table 5]. Here N represents the number of exercise dates. If N increases, then the Bermudan prices tend to those of their American counterpart. The lower part of Table 4 shows our approximations to the American put option prices using the FD discretization with fixed $m = 150$ and applying the MCS-IT method with $N = 20, 40, 60$ time steps. Clearly the prices obtained by both methods agree well, in particular those for the largest N .

Note that the values in the lower part of Table 4 could also be viewed as approximations to Bermudan put option prices with N exercise dates. The time step Δt is then equal to the full

period between two successive exercise dates. More accurate approximations to the Bermudan prices are (readily) obtained by reducing this time step.

	m_1	m_2	N	90	100	110
[9] FO			20	9.9784	3.2047	0.9274
			40	9.9916	3.2073	0.9281
			60	9.9958	3.2079	0.9280
MCS-IT	300	150	20	9.9984	3.2121	0.9301
	300	150	40	10.0015	3.2125	0.9304
	300	150	60	10.0039	3.2126	0.9305

Table 4: Parameter set (5.3), $S_0 \in \{90, 100, 110\}$, $V_0 = 0.0348$. Upper part: approximations to vanilla Bermudan put prices from [9]. Lower part: approximations to vanilla American put prices using MCS-IT method with $\theta = \frac{1}{3}$.

For future reference we give in Table 5 approximations for vanilla American put option prices in all six cases of Table 1 for spot asset prices $S_0 \in \{90, 100, 110\}$ and spot variance $V_0 = 0.05$. These have been computed using the FD discretization with $m = 250$ and the MCS-IT method with $\theta = \frac{1}{3}$ and $N = 125$. The full option price surfaces are displayed in Figure 5.

Case	90	100	110
A	16.9245	11.9442	8.2270
B	16.0470	12.4326	9.8746
C	10.4054	3.9235	1.1784
D	10.9554	8.6273	7.4999
E	12.8442	9.8116	8.4312
F	18.9325	15.6696	13.2838

Table 5: Vanilla American put option price approximations in all cases of Table 1 with $\rho \neq 0$ and $S_0 \in \{90, 100, 110\}$, $V_0 = 0.05$.

Next, Figure 6 shows for a selection of values $v \approx 0.002, 0.01, 0.05, 0.1, 0.24$ the corresponding parts of the free boundary in the (t, s) -plane. With the ADI-IT method proposed in this paper, the exercise and continuation regions are directly obtained by determining at each time point $t = t_n$ the two subsets of spatial grid points (s_i, v_j) where the corresponding component of the auxiliary vector $\widehat{\lambda}_n$ is strictly positive resp. equal to zero. The part below each curve in Figure 6 represents the exercise region and the part above the continuation region.

Finally, as a more exotic option we consider the capped American put option. This is an American-style option with a cap $B < K$ on the underlying asset price. If the asset price goes below the cap B , then the option is automatically exercised and an amount of $K - B$ is paid out to the holder. The relevant option value function u satisfies the Heston PDCP (1.3) whenever $s > B$, $v > 0$, $0 < t \leq T$ with ϕ given by (1.2). The boundary condition (2.1a) becomes

$$u(B, v, t) = K - B.$$

To numerically solve the Heston PDCP for a capped American put we follow the same approach as above in this paper, with spatial discretization given in Section 2 and for the time discretization the ADI-IT methods defined in Section 4. Only two minor modifications are needed: set

$$\xi_{\min} = \sinh^{-1} \left(\frac{B - S_{\text{left}}}{d_1} \right)$$

in the nonuniform mesh for the s -direction and modify S_{left} to $\max(\frac{1}{2}K, e^{-rT}K, B)$. The ROI is naturally truncated at $s = B$. As an illustration we consider cases C and E with nonzero correlation and cap $B = 80$. The left-hand side of Figure 7 displays the capped American put option price surfaces in these two cases. On the right-hand side of the figure, the temporal discretization errors $\hat{e}(\Delta t; 100, 50)$ for the four ADI-IT methods are shown. From these and additional experiments, we obtain similar, positive results concerning unconditional stability and stiff convergence as in the case of vanilla American put options.

6 Conclusions

We have proposed a simple, effective adaptation of ADI time discretization schemes to the numerical pricing via PDCPs of American-style options under the Heston model. The adaptation has been achieved by invoking a recent splitting idea due to Ikonen & Toivanen [26] and we refer to the acquired methods as ADI-IT methods. Four ADI-IT methods have been investigated in detail: Do-IT, CS-IT, MCS-IT and HV-IT. These are based on the Douglas, Craig–Sneyd, modified Craig–Sneyd and Hundsdorfer–Verwer schemes. The favorable result is found that, with properly chosen values for their parameter θ , all four methods show an unconditionally stable behavior in the application to a variety of representative, challenging test cases. Next, they all exhibit a satisfactory convergence behavior, provided Do-IT and CS-IT are used with a damping procedure. In all but one test cases, the MCS-IT and HV-IT methods, as well as the CS-IT method applied with damping, show a stiff order of convergence equal to two. They always yield about the same size temporal error for the same time step. In one test case the observed order was slightly lower, namely about 1.7, but this is still fine. The Do-IT method applied with damping was found to perform equally well as the other three methods for larger time steps, but for smaller time steps the (expected) lower convergence order of one sets in for this method whenever the correlation is nonzero. In view of the results in this paper, we recommend either the MCS-IT or HV-IT method in the numerical pricing of American options under the Heston model. Also the CS-IT method is a good candidate whenever it is used with damping.

A theoretical stability and convergence analysis of ADI-IT methods is still open at this moment. We proved a relevant, useful theorem for the BE-IT method, i.e. the backward Euler scheme combined with IT splitting. The ideas in this proof may be helpful for an analysis of ADI-IT methods in the future.

On the practical side, a comparison of the performance of the ADI-IT approach to other numerical techniques for the Heston PDCP is of much interest. This requires an extensive and careful study, however, and is left for future research. Nevertheless, from the discussion and results presented in this paper, we believe it is clear that ADI-IT methods are expected to be competitive.

Finally, a merit of the ADI-IT approach is the versatility: it is readily applicable in the case of many other underlying asset pricing models, other American-style options, or other semidiscretizations (by finite differences, volumes or elements) of the pertinent PDCPs.

Acknowledgements

This work has been supported financially by the Research Foundation – Flanders, FWO contract no. G.0125.08.

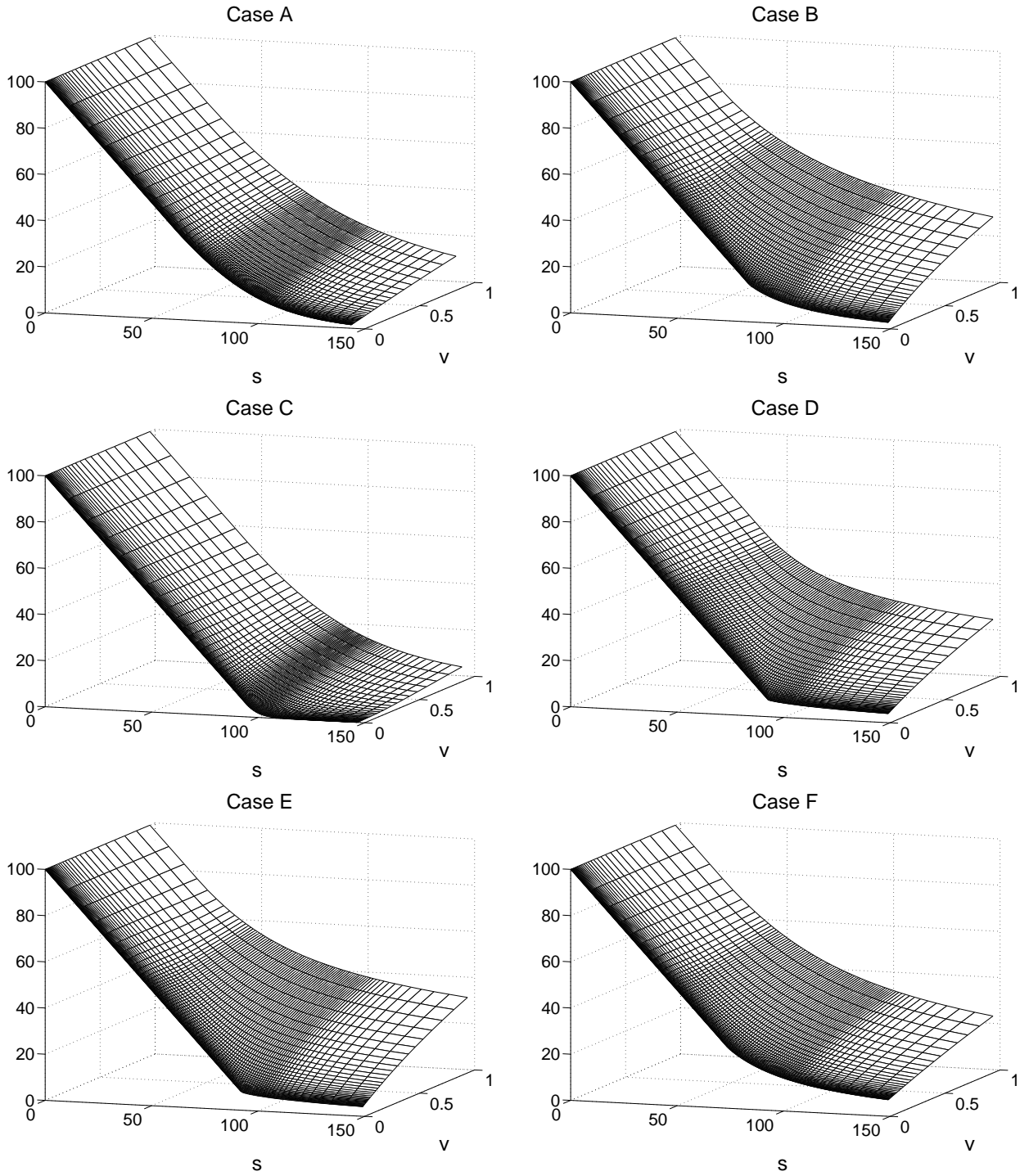


Figure 5: Approximated vanilla American put price surfaces in all cases of Table 1 with $\rho \neq 0$.

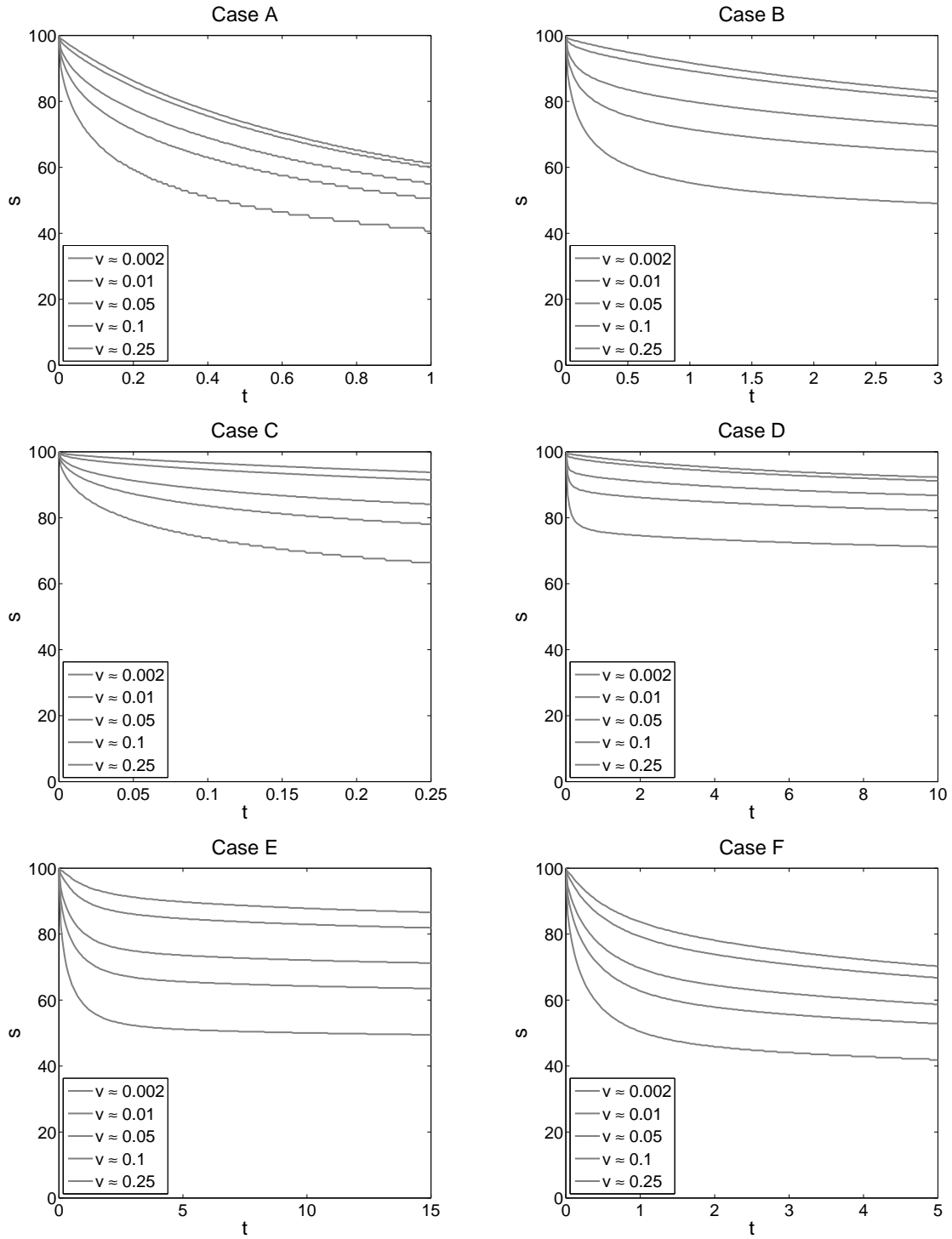


Figure 6: Approximated free boundaries for vanilla American put options in all cases of Table 1 with $\rho \neq 0$. From top to bottom: $v \approx 0.0021$, $v \approx 0.0093$, $v \approx 0.0484$, $v \approx 0.0972$, $v \approx 0.2392$.

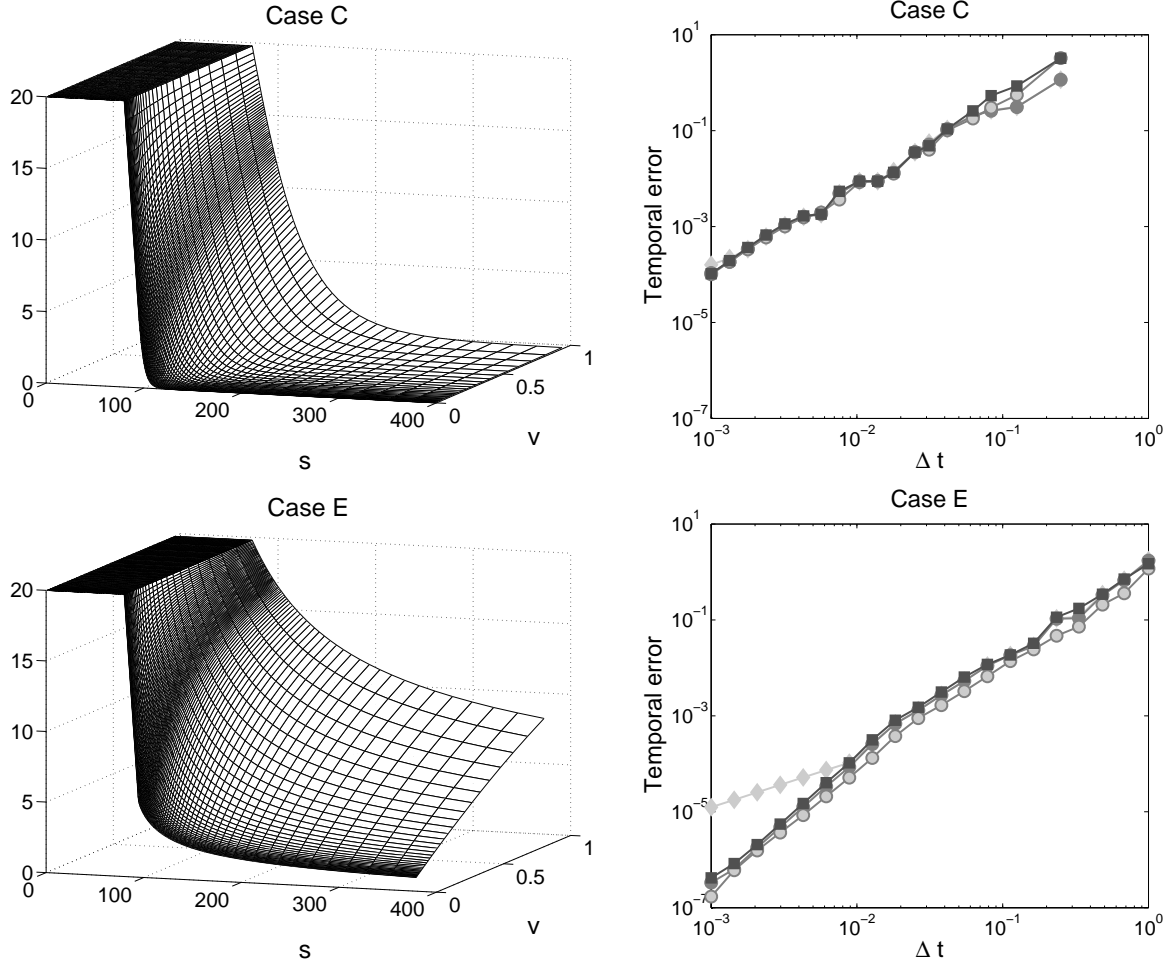


Figure 7: Capped American put options in cases C and E of Table 1 with $\rho \neq 0$ and cap $B = 80$. Left: Option price surfaces. Right: Temporal errors $\hat{e}(\Delta t; 100, 50)$ vs. Δt . Four ADI-IT methods: Do-IT with $\theta = \frac{1}{2}$ (light diamond), CS-IT with $\theta = \frac{1}{2}$ (dark circle), MCS-IT with $\theta = \frac{1}{3}$ (light circle) and HV-IT with $\theta = \frac{1}{2} + \frac{1}{6}\sqrt{3}$ (dark square). Do-IT and CS-IT with damping - two steps $\Delta t/2$ with BE-IT.

References

- [1] L. Andersen, *Simple and efficient simulation of the Heston stochastic volatility model*, J. Comp. Finan. **11** (2008) 1–42.
- [2] A. Berman & R. J. Plemmons, *Nonnegative Matrices in the Mathematical Sciences*, SIAM, Philadelphia, 1994.
- [3] Bloomberg Quant. Finan. Devel. Group, *Barrier options pricing under the Heston model*, 2005.
- [4] A. Brandt & C. W. Cryer, *Multigrid algorithms for the solution of linear complementarity problems arising from free boundary problems*, SIAM J. Sci. Stat. Comp. **4** (1983) 655–684.
- [5] M. J. Brennan & E. S. Schwartz, *The valuation of American put options*, J. Finan. **32** (1977) 449–462.
- [6] N. Clarke & K. Parrott, *The multigrid solution of two factor American put options*, Research Report 96-16, Oxford Computing Laboratory, Oxford, 1996.
- [7] N. Clarke & K. Parrott, *Multigrid for American option pricing with stochastic volatility*, Appl. Math. Finan. **6** (1999) 177–195.
- [8] I. J. D. Craig & A. D. Sneyd, *An alternating-direction implicit scheme for parabolic equations with mixed derivatives*, Comp. Math. Appl. **16** (1988) 341–350.
- [9] F. Fang & C. W. Oosterlee, *A Fourier-based valuation method for Bermudan and barrier options under Heston’s model*, SIAM J. Finan. Math. **2** (2011) 439–463.
- [10] R. Glowinski, *Finite element methods for incompressible viscous flow*, Handbook of Numerical Analysis, vol. 9, eds. P. G. Ciarlet & J. L. Lions, Elsevier, Amsterdam, 2003.
- [11] T. Haentjens, *Efficient and stable numerical solution of the Heston–Cox–Ingersoll–Ross partial differential equation by alternating direction implicit finite difference schemes*, Int. J. Comp. Math., published online (2013), DOI: 10.1080/00207160.2013.777710.
- [12] T. Haentjens & K. J. in ’t Hout, *Alternating direction implicit finite difference schemes for the Heston–Hull–White partial differential equation*, J. Comp. Finan. **16** (2012) 83–110.
- [13] T. Haentjens, K. J. in ’t Hout & K. Volders, *ADI schemes with Ikonen–Toivanen splitting for pricing American put options in the Heston model*, In: Numerical Analysis and Applied Mathematics, eds. T. E. Simos et. al., AIP Conf. Proc. **1281** (2010) 231–234.
- [14] E. Hairer & G. Wanner, *Solving Ordinary Differential Equations II*, 2nd ed., Springer, Berlin, 2002.
- [15] S. L. Heston, *A closed-form solution for options with stochastic volatility with applications to bond and currency options*, Rev. Finan. Stud. **6** (1993) 327–343.
- [16] K. J. in ’t Hout & S. Foulon, *ADI finite difference schemes for option pricing in the Heston model with correlation*, Int. J. Numer. Anal. Mod. **7** (2010) 303–320.
- [17] K. J. in ’t Hout & C. Mishra, *Stability of the modified Craig–Sneyd scheme for two-dimensional convection-diffusion equations with mixed derivative term*, Math. Comp. Simul. **81** (2011) 2540–2548.
- [18] K. J. in ’t Hout & K. Volders, *Stability of central finite difference schemes for the Heston PDE*, Numer. Algor. **60** (2012) 115–133.
- [19] K. J. in ’t Hout & B. D. Welfert, *Stability of ADI schemes applied to convection-diffusion equations with mixed derivative terms*, Appl. Numer. Math. **57** (2007) 19–35.

- [20] K. J. in 't Hout & B. D. Welfert, *Unconditional stability of second-order ADI schemes applied to multi-dimensional diffusion equations with mixed derivative terms*, Appl. Numer. Math. **59** (2009) 677–692.
- [21] J. Huang & J.-S. Pang, *Option pricing and linear complementarity*, J. Comp. Finan. **2** (1998) 31–60.
- [22] W. Hundsdorfer & J. G. Verwer, *Numerical Solution of Time-Dependent Advection-Diffusion-Reaction Equations*, Springer, Berlin, 2003.
- [23] S. Ikonen & J. Toivanen, *Operator splitting methods for American option pricing*, Appl. Math. Lett. **17** (2004) 809–814.
- [24] S. Ikonen & J. Toivanen, *Componentwise splitting methods for pricing American options under stochastic volatility*, Int. J. Theor. Appl. Finan. **10** (2007) 331–361.
- [25] S. Ikonen & J. Toivanen, *Efficient numerical methods for pricing American options under stochastic volatility*, Numer. Meth. Part. Diff. Eq. **24** (2008) 104–126.
- [26] S. Ikonen & J. Toivanen, *Operator splitting methods for pricing American options under stochastic volatility*, Numer. Math. **113** (2009) 299–324.
- [27] S. McKee & A. R. Mitchell, *Alternating direction methods for parabolic equations in two space dimensions with a mixed derivative*, Computer J. **13** (1970) 81–86.
- [28] S. McKee, D. P. Wall & S. K. Wilson, *An alternating direction implicit scheme for parabolic equations with mixed derivative and convective terms*, J. Comp. Phys. **126** (1996) 64–76.
- [29] C. W. Oosterlee, *On multigrid for linear complementarity problems with application to American-style options*, Elec. Trans. Numer. Anal. **15** (2003) 165–185.
- [30] D. W. Peaceman & H. H. Rachford, *The numerical solution of parabolic and elliptic differential equations*, J. Soc. Indus. Appl. Math. **3** (1955) 28–41.
- [31] J. Persson & L. von Sydow, *Pricing American options using a space-time adaptive finite difference method*, Math. Comp. Simul. **80** (2010) 1922–1935.
- [32] W. Schoutens, E. Simons & J. Tistaert, *A perfect calibration! Now what?*, Wilmott mag., March 2004, 66–78.
- [33] D. Tavella & C. Randall, *Pricing Financial Instruments*, Wiley, New York, 2000.
- [34] J. Toivanen & C. W. Oosterlee, *A projected algebraic multigrid method for linear complementarity problems*, Numer. Math. Theor. Meth. Appl. **5** (2012), 85–98.
- [35] M. Vellekoop & H. Nieuwenhuis, *A tree-based method to price American options in the Heston model*, J. Comp. Finan. **13** (2009) 1–21.
- [36] S. Villeneuve & A. Zanette, *Parabolic ADI methods for pricing American options on two stocks*, Math. Oper. Res. **27** (2002) 121–149.
- [37] P. Wilmott, J. Dewynne & S. Howison, *Option Pricing: Mathematical Models and Computation*, Oxford Financial Press, Oxford, 1995.
- [38] G. Winkler, T. Apel & U. Wystup, *Valuation of options in Heston's stochastic volatility model using finite element methods*, Foreign Exchange Risk, eds. J. Hakala & U. Wystup, Risk Books, London (2002) 283–303.
- [39] R. Zvan, P. A. Forsyth & K. R. Vetzal, *Penalty methods for American options with stochastic volatility*, J. Comp. Appl. Math. **91** (1998) 199–218.